Monte Carlo calculations in comparison to neutron scattering studies: 2. Global dimensions of 12-arm stars

Klaus Huber, Walther Burchard, Siegfried Bantle* and Lewis J. Fetters†
Institute of Macromolecular Chemistry, University of Freiburg, D-7800 Freiburg, FRG
(Received 29 October 1986; revised 25 March 1987; accepted 19 June 1987)

Light and neutron scattering studies were carried out on 12-arm star polystyrene molecules in toluene (a good solvent) and in cyclohexane (a θ-solvent). The polymers had a molecular weight range of $5 \times 10^4 < M_w < 1.6 \times 10^6$. The global dimensions of all samples under θ conditions are larger than those predicted by the existing theories. Monte Carlo simulations of 12-arm star chains as a function of chain length were performed using Flory's rotational isomeric state model. Two different types of star chains, a pure combinatorial star and a star with a specific centre were used. These aided the interpretation of the experimental results.

(Keywords: light scattering; neutron scattering; 12-arm polystyrene; theta conditions; Monte Carlo calculations; rotational isomeric state model)

INTRODUCTION

The overall dimensions of regularly branched molecules are expected to be smaller than those of the corresponding linear chains. This decrease in dimensions, often termed 'shrinking', becomes increasingly significant if the number of arms f increases. One common measure of shrinking is the ratio g of the squared radius of gyration $\langle S^2 \rangle_b$ of the star molecule and the squared radius of gyration of the respective linear chain $\langle S^2 \rangle_l$ at the same molecular weight

$$g = \langle S^2 \rangle_b / \langle S^2 \rangle_l \quad (1)$$

Assuming a Gaussian distribution of intramolecular distances, Zimm and Stockmayer derived the first analytical expression for g,[1]

$$g = (3f - 2)/f^2 \quad (2)$$

31 years later Mansfield and Stockmayer[2] expanded the theory of star dimensions to include the worm-like chain model of Kratky and Porod[3]. Their main result was a molecular weight dependent g-ratio, which, for short chains is smaller than the Gaussian limit (equation (2)). However, if the chains are sufficiently long the value of g approaches that of equation (2).

For an investigation of the overall dimensions of star molecules, scattering experiments seem to be most convenient. In many previous papers, the geometry of star molecules was the subject of light scattering (LS) experiments[4-9]. Recently a paper with X-ray scattering results on the same subject was published[10]. If the number of arms is greater than 6 the shrinking factors determined by those experiments are significantly larger than those predicted by equation (2). However, the small overall dimensions of stars, especially in the case of a high degree of branching, limited somewhat the application of light scattering. In a more recent paper, we investigated polystyrene (PS) 12-arm star molecules over an extended range of molecular weights[11] ($5.5 \times 10^4 < M_w < 1.7 \times 10^6$) where a molecular weight dependence of the shrinking behaviour was indeed observed. The static LS results were relatively inaccurate in the lower molecular weight range, and for the smallest sample PS 9–12, $\langle S^2 \rangle_b$ could not be determined[11]. We therefore performed small-angle neutron scattering (SANS) experiments with the three lowest 12-arm star samples: PS 9–12, PS 6–12 and PS 4–12, both in toluene-d_8 and cyclohexane-d_{12}. With these supplementary experiments, a more accurate and extensive picture of the molecular weight dependence of star dimensions has been obtained.

Another method of describing polymer structures, which is quite different from analytical approaches, is to simulate polymeric chains according to the well known Monte Carlo procedure. This method, which was very successful for linear chains, has been extended to regular star branched chains during the past ten years[12-17]. If excluded volume effects were explicitly taken into account by self-avoiding chains, the g values of the simulated chains are slightly larger than predicted by equation (2)[12,14,17]. This behaviour is comparable with the experimentally determined results.

SANS MEASUREMENTS

Measurements were performed at the Institut Max von Laue–Paul Langevin (ILL), Grenoble, France. All experiments were carried out with the D-17 instrument, where a 64×64 cell matrix assembly[18] was used for detecting the scattering intensity. The detector was positioned at an angle of 3°. The wavelength of the neutrons was 1.0 nm. For determining $\langle S^2 \rangle_z$, a sample detector distance of 2.7 m was chosen. Sample PS 4–12,

* Institut Laue–Langevin, Grenoble, France; present address: Sandoz AG, Basle, Switzerland.
† Present address: Corporate Research–Science Laboratories, Exxon Research and Engineering Co., Annandale, NJ 08801, USA.

0032-3861/87/121990-07$03.00

Table 1 SANS results for the PS 12-arm star molecules in toluene-d_8 at 20°C and in cyclohexane-d_{12} at 35°C

Sample	$M_w \times 10^3$	$\langle S^2 \rangle_z$ (nm^2)	
		Toluene-d_8	Cyclohexane-d_{12}
PS 9–12	54	14.7	15.1
PS 9–12			15.2[a]
PS 6–12	149	53.3	48.6
PS 4–12	423	161	137

[a] Measured at $T = 28$°C

with the highest molecular weight, was in addition measured with the D-11 instrument. Radial averaging and data treatment were performed at ILL[19]. Further details of the SANS measurements are published in the preceding paper, that dealt with linear chains[20]. The solvents cyclohexane-d_{12} and toluene-d_8 were used without further purification (98% D; from Merck, Sharp and Dohme, Canada).

SANS measurements were performed with three different PS 12-arm star samples (*Table 1*). A plot of $(K_c/R_\theta)^{1/2}$ *versus* q^2 (Berry plot[32]) gave straight lines over a wide q^2 region[33] and allowed a highly reliable determination of the radius of gyration $R_g \equiv \langle S^2 \rangle^{1/2}$. The accuracy was further increased by determining the maximum position of the scattering intensity in the Kratky plot. This maximum occurs for Gaussian chains at a well defined position of $u_{max} = R_g q_{max}$. Details are described in part 3 of this series, (see following paper). All samples were synthesized according to a procedure, which is described elsewhere[10]. The polydispersity index M_w/M_n in all three cases was smaller than 1.1. LS results from the samples have already been published in ref. 10.

A main problem within these experiments was to choose a convenient temperature for the measurements in the θ-solvent cyclohexane-d_{12}. As was pointed out by Strazielle *et al.*[21], the θ-point of PS in deuterated cyclohexane is about 4°C higher than that in cyclohexane. On the other hand, in the molecular weight range $M_w < 5 \times 10^5$, the temperature, where $A_2 = 0$ for 12-arm star molecules, is significantly lower than for linear chains[7,10]. The SANS measurements in cyclohexane-d_{12}, published in the present paper were performed at $T = 35$°C. This is the same temperature as used for the LS experiments[10] in cyclohexane. In addition $T = 35$°C was the temperature where K_c/R_θ values for the sample PS 4–12 in cyclohexane-d_{12} were concentration independent. To look for temperature dependent changes in the dimensions, we repeated the SANS measurements for the smallest sample, PS 9–12, at a lower temperature of $T = 28$°C, where again we had $A_2 = 0$. As can be seen from *Table 1*, no significant change in $\langle S^2 \rangle_b$ is observed.

Determination of $\langle S^2 \rangle_b$ was extremely accurate and the error was less than 6%. The molecular weights, determined by SANS measurements, are in good agreement with ref. 11.

MONTE CARLO CALCULATIONS

In addition to the SANS experiments, we performed Monte Carlo simulations of 12-arm polymethylene (PM) star chains on the basis of the rotational isomeric state (r.i.s.) model of Flory[22]. This procedure, which was first applied by Yoon *et al.*[23] starts from the matrix, containing the *a priori* probabilities p

$$\mathbf{P} = \begin{pmatrix} 0.321 & 0.138 & 0.138 \\ 0.138 & 0.059 & 0.0052 \\ 0.138 & 0.0052 & 0.059 \end{pmatrix} \quad (3)$$

for the rotational angle of a bond, being in the η state, supposing that the preceding bond is in the ξ state. Equation (3) fixes PM in its unperturbed dimensions. $\chi = 0$, $+120°$ and $-120°$ were used as rotational isomeric states. The C–C bond length was 1.53 nm and the valence angle 112°.

By applying a random numbers generator to the matrix in equation (3), one gets a sequence of rotational isomeric states of carbon backbone bonds, which determines the conformation of a polymeric chain. Details of the calculation procedure are given in the paper on linear chains[20], the results of which will be used as reference material for a comparison with the star branched molecules.

To characterize a polymeric chain of a certain number of skeletal ataoms n_A, at least 1000 different conformers were generated. As detailed below, two different methods of constructing the 12-arm star molecules were followed.

Combinatorial star

First, linear chains were generated, following exactly the procedure described in ref. 20. Within this procedure the conformers data were stored in histograms containing the distance distributions of sub-chains. These histograms enabled us to calculate the double sums of atom–atom pair combinations ij, leading to the mean square radius of gyration $\langle S^2 \rangle$;

$$\langle S^2 \rangle = (1/2n_A^2) \sum_i^{n_A} \sum_j^{n_B} \langle r_{ij}^2 \rangle \quad (4)$$

the hydrodynamic radius R_h;

$$1/R_h = (1/n_A) \sum^{n_A} \sum^{n_B} \langle 1/r_{ij} \rangle \quad (5)$$

and the particle scattering factors of the polymeric chains (to be dealt with in the succeeding paper). Here $\langle r_{ij}^2 \rangle$ is the mean square distance and $\langle 1/r_{ij} \rangle$ the reciprocal mean distance between atoms i and j. In order to emulate star-like behaviour, the linear chains were regarded as a part of the 12-arm star molecule, consisting of the star centre (the backbone atom in the midst of the chain) and two arms. The resulting double sums were split up into three parts with different pair combinations, which were weighted by different factors (*Figure 1*); i.e.

(i) Intra-arm combinations cover all distances within the same arm; the weighting factor for this type amounts to f.

(ii) Inter-arm combinations, where the atoms of each pair belong to two different arms; the weighting factor now amounts to $f(f-1)$.

(iii) Combinations between the star centre and each backbone atom. This type is weighted by the factor $f/2$.

As a main feature, the arms of the combinatorial star contain no correlation of their initial directions in the star centre. This combinatorial star should approach the

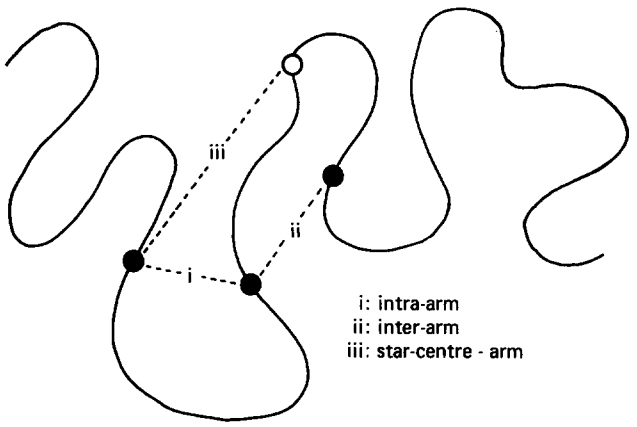

Figure 1 Schematic representation of the combinatorial star model

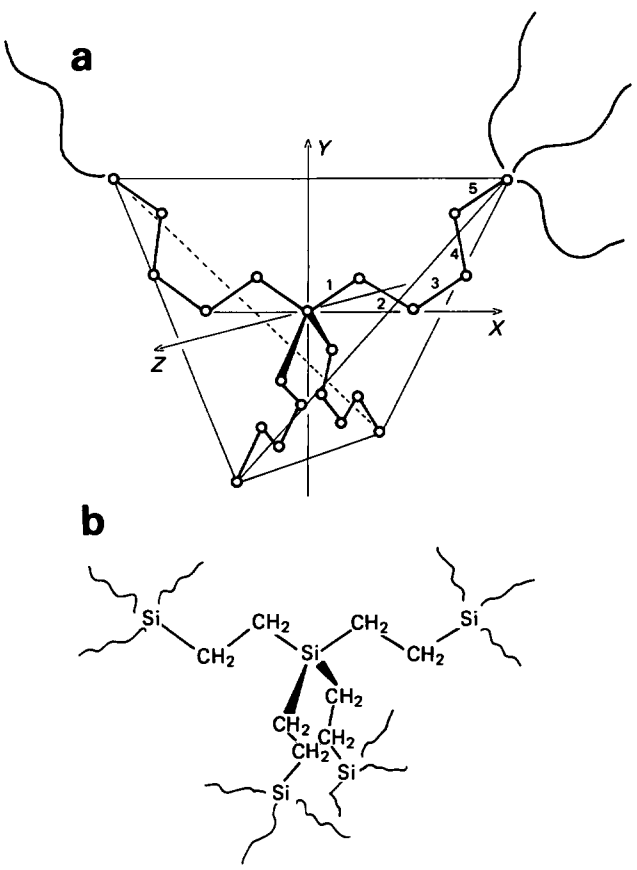

Figure 2 (a) Model of the specific star centre, which was used for the Monte Carlo simulations; the empty circles are carbon backbone atoms. (b) Star of the PS 12-arm star molecules used in this work and elsewhere[7-9,11]

results of the worm-like star model[2] *with no* correlation between the arms, provided the arms are significantly longer than the Kuhn segment length l_K of a PM chain[20]. A remarkable advantage of this combinatorial star is that the generation of two arms is sufficient to produce all the information about the whole star molecule. The principles of the combinatorial star are already included implicitly in the Gaussian star model of Zimm and Stockmayer[1].

Star with a specific centre

In the second procedure, a specific star centre is used. This centre consists of four short linear chains which are linked together tetrahedrically at one point (*Figure 2a*). Each free end of these short sub-chains is the starting point of three arms. The length of 5 bonds for the central sub-chains enabled us to form a tetrahedral symmetry of the free chain ends if the rotational isomeric states of bond 2, 3 and 4 in each sub-chain were fixed to *trans* (0°), eclipsed (180°) and *trans* (0°) respectively, (*Figure 2a*). Due to the introduction of this specific star centre, the intramolecular distances r_n between two atoms i and j now depend on the special location within the chain. For this reason, an application of the histogram method[11] was no more acceptable, because not only for each $n=|j-i|$, but for all combinations ij with $j>i$, a histogram was required. Therefore $\langle S^2\rangle$, R_h and the particle scattering factor were calculated for each conformation and summed up, leading finally to the desired mean values. *Table 2* represents schematically the construction of the star molecules. The first column contains the chain segments providing backbone atoms for the pair combinations. Arabic numbers are used to sign arms and roman numbers to sign central sub-chains. The second column gives the weighting factors for the respective type of pair combinations. The third column contains the generated chain segments, encircled numbers denote the last segment which was added. In principle, the special symmetry of the star centre made it possible to confine ourselves to the generation of four arms, i.e. three arms at one tetrahedral edge and one at a second edge. Nevertheless the procedure described in *Table 2* where we generated the additional arms 5 and 6, consumed less storage.

This model of a specific star centre consists of a special and very unlikely sequence of rotational angles. Nevertheless, for two reasons we think that this model yields valuable information on the influence of a star

Table 2 Successive construction of the star conformer with the specific star centre

Combination	Weighting	Generated parts
I with I	1	
II with II	3	
I with II	6	
1 with 2	18	
1 with 1	3	1—I—II—2
2 with 2	3	
1 with I	3	
1 with II	9	
2 with II	3	
1 with II	9	
1 with 3	18	
3 with 3	3	
3 with II	3	1—I—II(3), 2
3 with I	9	
1 with 4	18	
4 with 4	3	
4 with II	3	1—I—II(4), 3, 2
4 with I	9	
1 with 5	4	(5), I—II, 1, 2, 3, 4
1 with 6	4	(6), 5, I—II, 1, 2, 3, 4
5 with 6	4	

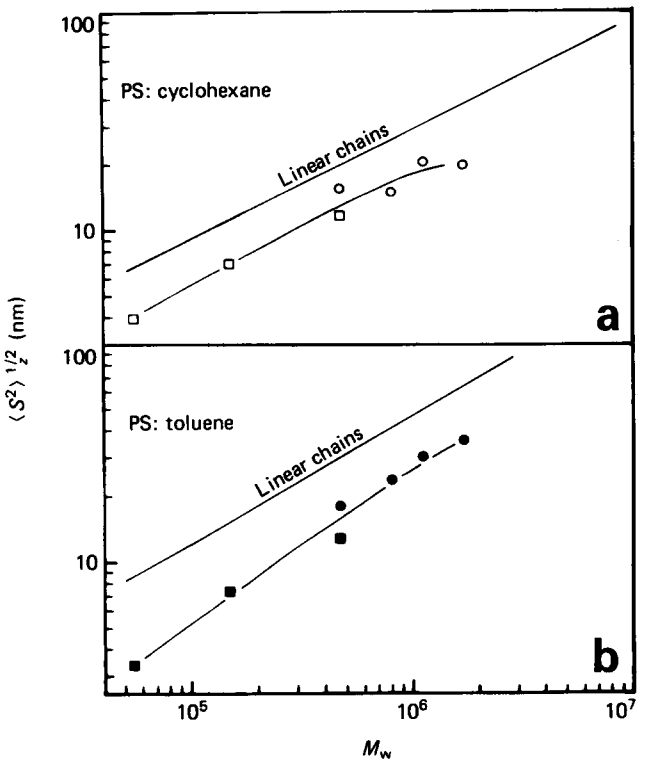

Figure 3 $\langle S^2 \rangle_z^{1/2}$ for PS 12-arm stars in cyclohexane (a) and toluene (b) as function of molecular weight; circles stand for LS experiments and squares for SANS experiments in deuterated solvents

centre onto the global dimensions and the particle scattering factor. Firstly, like the 12-arm star molecules used in the work by Fetters[11] and elsewhere[7-10] (*Figure 2b*), this model contains an extended star centre of four short sub-chains. Secondly, like a characteristic feature of real star molecules, our model has a correlation of the directions of the arms emanating from the centre.

DECREASE OF THE GLOBAL DIMENSIONS

Figure 3a,b exhibits the molecular weight dependence of $\langle S^2 \rangle_b^{1/2}$ for PS 12-arm star molecules, both in toluene and cyclohexane. To discuss the decrease of $\langle S^2 \rangle_b$ with respect to linear PS quantitatively, we turn to the experimental g factors. The $\langle S^2 \rangle_l$ values, required for the deviation of these g factors, in cyclohexane were taken from equation (6) of ref. 24. The result is shown in *Figure 4* together with the predictions of the Gaussian[1] and worm-like[2] star models. According to equation (2) one has $g = 0.236$, independent of molecular weight. To calculate g of the worm-like star chains[2] we used the chain parameters l_K and m_l (Kuhn length and mass per unit length) of PS in cyclohexane[20]. The initial directions of the arms of the worm-like star chain at the star centre are considered to be totally correlated[2].

The experimentally determined g factors, for all molecular weights, are higher than predicted by any theory. They are, however, in fair agreement with the results, obtained from similar PS 12-arm star molecules in methyl-ethyl-ketone[10]. However, one gets the impression that the experimental g factor approaches the theoretical prediction if the molecular weight is sufficiently high. The most striking feature in *Figure 4* is the fact that g, according to the worm-like chain model, seems to describe the experimental behaviour less successfully than the Gaussian model.

To interpret these results, one has to keep in mind that both the Gaussian and the worm-like chain model are based on the following assumption. The star molecule is built up of linear chains, which retain their structure when they are 'inserted' into the star. Such an assumption is rather questionable with regard to the specific properties of the star centre. This centre fixes the linear chains on one end and produces a high segment density. These two star centre characteristics will lead to further stretching relative to the free chains and causes the increase in g for the PS star molecules. Equivalent chain stiffness of arms within the star and of linear reference chains would always lead to g values smaller than that of the Gaussian model ($g = 0.236$). In the limit of rigid rods g even approaches the value of 0.0278 (ref. 2) if $f = 12$.

A comparison of all measured g values[4-8,11] with the theoretical function of $g(f)$ in equation (2) yields good agreement up to $f = 6$,[11] if the data of the respective highest molecular weight were used. For larger f, theory and experiment diverge. The molecular weight range, where the experimental g approaches equation (2), is shifted towards higher molecular weights if f is increased. For $f < 6$, the experimentally available molecular weights have already reached this range.

SIMULATED STAR CHAINS

The results of the Monte Carlo calculations are summarized in *Tables 3* and *4*. *Figure 5* gives a graphic

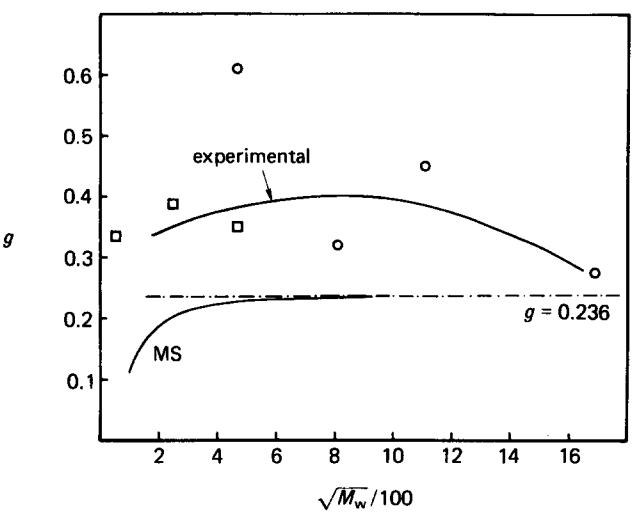

Figure 4 g ratios for the PS 12-arm star molecules in cyclohexane; (MS) worm-like star chains according to Mansfield and Stockmayer[2]; (experimental) interpolated curve for the experimental data; ($g = 0.236$) Gaussian coil limit. Symbols as in *Figure 3a*

Table 3 $\langle S^2 \rangle^{1/2}$ and R_h of the combinatorial star chains generated with the r.i.s.–Monte Carlo procedure

Probe	n_B	$\langle S^2 \rangle^{1/2}$ (nm)	R_h (nm)
STK01	60	0.4422	0.5015
STK02	144	0.7999	0.8159
STK03	180	0.9173	0.9174
STK04	372	1.437	1.345
STK05	480	1.667	1.532
STK07	1224	2.730	2.424

Table 4 $\langle S^2\rangle^{1/2}$ and R_h of the star chains with a specific star centre generated with the r.i.s.–Monte Carlo procedure

Probe	n_B	$\langle S^2\rangle^{1/2}$ (nm)	R_h (nm)
STR1	56	0.6423	0.6235
STR5	92	0.7974	0.7732
STR3	140	0.9649	0.9315
STR2	176	1.078	1.038
STR4	368	1.534	1.445
STR6	476	1.756	1.631
STR7	1220	2.820	2.536

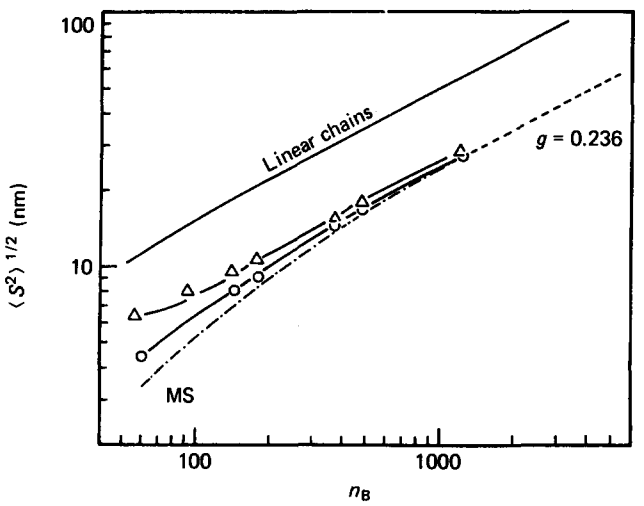

Figure 5 Monte Carlo simulations on 12-arm star chains: (○) combinatorial star chains; (△) star chains with a specific star centre; (–·–·–) worm-like star chains without a correlation between the initial directions of any two arms[2]; (– – –) Gaussian coil limit. The data on linear PM r.i.s.-chains are from ref. 19

representation of those results together with the data for linear PM chains which were taken from ref. 19. The triangles correspond to the star chains with a specific star centre and the circles to the combinatorial star chains. As can be seen from *Figures 5* and *6* the worm-like chain model according to Mansfield and Stockmayer[2] is a good approximation to the combinatorial r.i.s.-star chains, if the number of bonds is not too low. The theoretical behaviour of the star chains according to Mansfield and Stockmayer[2] as well as that of the combinatorial star chains are governed by a position-independent chain stiffness alone, and therefore the g ratios approach the Gaussian model from below.

In *Figures 5* and *6* we have used the worm-like star model by Mansfield and Stockmayer[2] as the reference for our r.i.s. model simulations which contain no correlation between the initial directions of the arms. However, according to Mansfield and Stockmayer[2] there is no difference in the global dimensions between models with and without a correlation between the initial directions of arms if f is as high as 12.

The deviations of the combinatorial star chains from the worm-like chain model of Mansfield and Stockmayer[2], in the low molecular weight regime, is caused by the following shortcoming of the combinatorial r.i.s. star chains. Whilst in the worm-like star, without correlation between the initial directions of the arms, all angles at the star centre have equal probabilities, for the discrete r.i.s. combinatorial star one has at least the bond angle of 112°. This restriction becomes noticeable if the arm length is decreased to a few Kuhn segment lengths. Due to the fact that the angle between the initial directions of any two arms cannot be less than 112°, the intramolecular distances within the direct neighbourhood of the star centre become larger on average.

The g factors of the star chains with a specific star centre approach the Gaussian behaviour from above. Now, two competing effects exist: (i) the original chain stiffness of arm and linear reference chain decreases the g-value; (ii) the extended star centre, consisting of four short arms with four further branching centres increases the g value. Clearly even in the case of 1220 bonds, the second effect dominates the first. Nevertheless, the deviations are not as pronounced as in the case of the PS 12-arm star molecules (*Figures 5* and *6*) because the generated arms are not self-avoiding and the high segment density around the star centre therefore was not taken into account.

A few years ago, Mattice and Carpenter[25,26] published calculations on 3- and 4-arm star chains, where a carbon backbone was based on five different *a priori* probability matrices **P**. The arms were linked together in a common point using the tetrahedral bond angles of the C-atom. In addition, the specific torsional potentials around the star centre were taken into account by changing **P** near the centre[25].

As already pointed out by Mattice and Carpenter[26], g approaches the Gaussian value from below, if the characteristic ratio C (as defined in ref. 25)

$$C=\langle S^2\rangle/(n_B b^2) \tag{6}$$

of the corresponding linear reference chains is smaller than 1. Here $\langle S^2\rangle$ is the mean square radius of gyration, b the bond length and n_B the number of backbone bonds. The special sequence of the rotational angles at the star centre is effected by the change of **P**. Clearly, only when $C<1$, will this lead to an additional stretching of the corresponding chain segments with respect to the linear reference chains.

EXCLUDED VOLUME EFFECTS

The influence of solvent behaviour onto the g ratio is shown in *Figure 7*, where g values in cyclohexane and toluene were plotted together. To calculate the g ratios in toluene, we used the experimental $\langle S^2\rangle_l$ dependence on M_w, published in ref. 27. As can be seen from *Figure 7*, the g values in toluene are well below those in cyclohexane, if

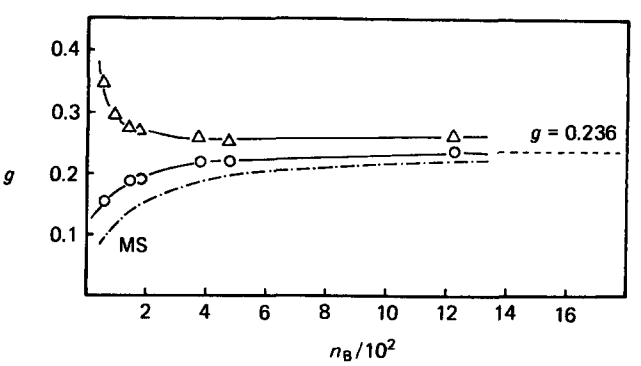

Figure 6 Curves of g *versus* M_w according to Monte Carlo calculations. Symbols as in *Figure 5*

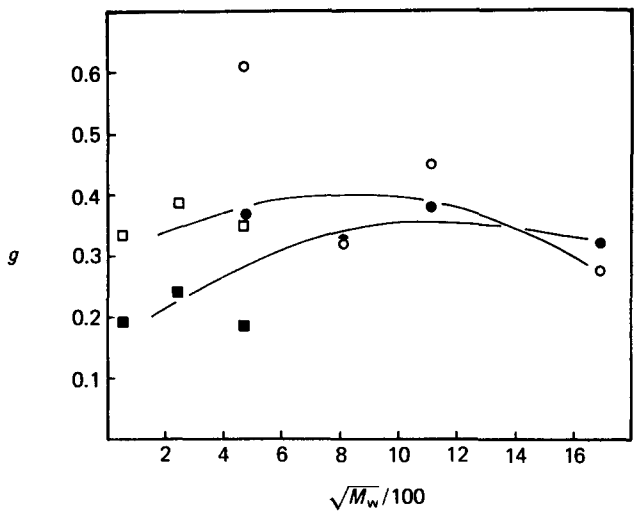

Figure 7 g ratios for PS 12-arm star molecules in toluene (●, ■) and cyclohexane (○, □). Symbols as in *Figure 3*

$M_w < 5 \times 10^5$. This decrease can be explained by the stretching of the arms in the star and, even more so, by the stretching of the linear reference chains by changing the solvent from cyclohexane to toluene.

To achieve a deeper insight into the effect of the good solvent, we used a plot of $g(\alpha)$ *versus* M_w

$$g(\alpha) \equiv \alpha_{sb}^2/\alpha_{sl}^2 = g_{Tol}/g_{Cyc} \tag{7}$$

This plot had already been suggested in an earlier paper[11] but is now supplemented with the SANS results. Here α_{sb} is the expansion of $\langle S^2 \rangle_b$ and α_{sl} the corresponding expansion for $\langle S^2 \rangle_l$. The theoretical course of $g(\alpha)$ can be calculated on the basis of the current theories on excluded volume effects. According to the procedure suggested by Yamakawa[28], one obtains the drawn curve of *Figure 8*. As a consequence of the enhanced segment density within the star molecule, the expansion α_{sb} is larger than the corresponding α_{sl}.

The experimental data in the low molecular weight regime are significantly below the above-mentioned theoretical prediction. In this molecular weight regime, the star molecules under θ conditions are already stretched out to a large extent and only minor extension takes place as a result of the interaction with the good solvent. At the lowest molecular weights, the experimental data merge into the dashed curve (*Figure 8*), which is calculated under the assumption, that $\alpha_{sb} = 1$, i.e. no further expansion due to the good solvent occurs within the star molecules. With increasing molecular weight, the portion of the star molecule which is made up by the star centre decreases and therefore the ability to expand, increases. The theoretical predictions seem therefore to be approached in the very high molecular weight range.

THE ρ-RATIO

According to Kirkwood and Riseman[31] the hydrodynamic radius R_h is defined as

$$1/R_h = 1/(n_k a_h) = 2(6/\pi)^{1/2}/(l_k n_k^2) \sum_{n=1}^{n_k} (n_k - n) n^{-1/2} \tag{8}$$

with n_k the number of statistical segments of size l_k and hydrodynamic radius a_h. The radius R_h, calculated with our Monte Carlo procedure corresponds to the -1st moment of the chain and therefore only contains the non-draining part of the hydrodynamic radius[20]. In the discussion of the limiting behaviour at $n_B \to \infty$, we confine ourselves to where the first or draining part of equation (7) could be neglected. To this end, we use the well known ρ-ratio

$$\rho = \langle S^2 \rangle^{1/2}/R_h \tag{9}$$

which for Gaussian star chains becomes[29]

$$\rho = [(3f-2)/(f\pi)]^{1/2} 8(2 - f + \sqrt{2}(f-1)/(3f)) \tag{10}$$

In the case of $f = 12$, the ρ-ratio is calculated to be 1.173, which is about 30% lower than for linear chains. With PS 12-arm stars, indeed a decrease of about 30% was observed[11]. However, for both the star molecules and the linear chains[11,24,30], the experimental ρ-ratios are significantly lower than predicted by theory[29,31]. The Monte Carlo simulations on the other hand yield ρ-data, the extrapolation of which towards $n_B \to \infty$ leads to ρ-values (*Figure 9*) in full agreement with equation (10). We finish by saying that the situation here is analogous to that for linear r.i.s. chains[20].

CONCLUSIONS

If a free linear chain is identical to a chain linked as an arm within a star molecule, theoretically there are two cases:

(1) The Gaussian chain structure has a constant g value, which is a function of f alone.

(2) The semiflexible chain structure produces g values which increase with molecular weight. These approach the g value of case (1) in the limit of very high molecular weight.

Several different effects given below superimpose themselves on consideration (2). They all increase the g-ratio:

(i) Fixed bond angles cause a correlation between the initial directions of the arms in the star centre. This effect is only important[2] for low f and low M_w.

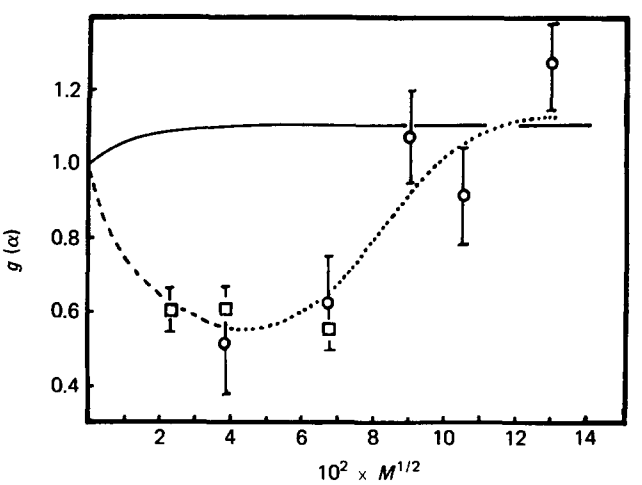

Figure 8 $g(\alpha)$ as function of M_w; (○) LS-data, (□) SANS data, (·····) fit of the experimental data, (– – –) calculation with $\alpha_{sl} = 1$, (———) theoretical curve for the Gaussian model

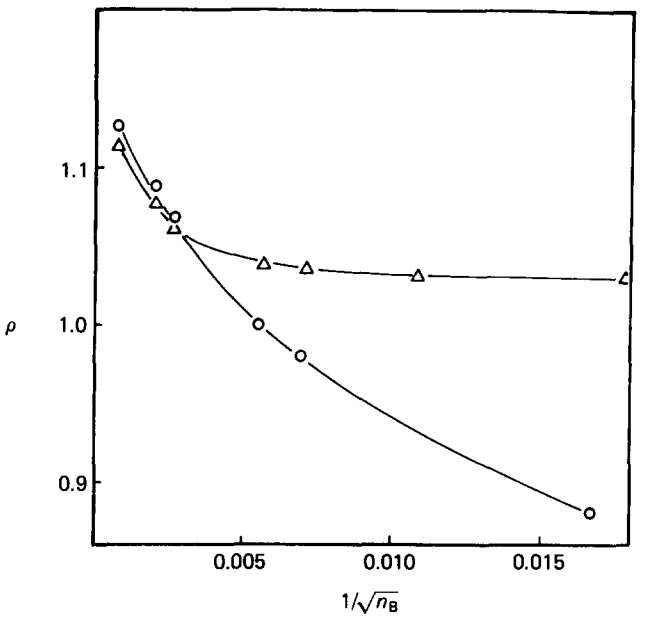

Figure 9 ρ-ratio of the r.i.s. 12-arm star chains; (○) combinatorial star chains; (△) star chains with a specific centre

(ii) If the number of arms is larger than 4, the arms cannot be linked together at one point any more. An extended star centre with several branching points is then necessary.

(iii) A relatively high segment density exists around the star centre. This high segment density causes an extraordinary stretching of the arms, since the arms are fixed at one of their ends within the star centre. This stretching, which decreases with increasing distance from the centre of the star, could be described by a model using a persistence length depending on the position along the arm. With increasing distance from the star centre chain stiffness decreases and assumes the value of the free chain if the position is far away from the centre.

ACKNOWLEDGEMENT

We would like to thank the Institut Max von Laue–Paul Langevin for the use of their neutron scattering facilities. The work was supported by the Deutsche Forschungsgemeinschaft within the scheme of SFB 60.

REFERENCES

1 Zimm, B. H. and Stockmayer, W. H. *J. Chem. Phys.* 1949, **17**, 1301
2 Mansfield, M. L. and Stockmayer, W. H. *Macromolecules* 1980, **13**, 1713
3 Kratky, O. and Porod, G. *Rec. Trav. Chim.* 1949, **68**, 1106
4 Roovers, J. E. L. and Bywater, S. *Macromolecules* 1972, **5**, 385
5 Roovers, J. E. L. and Bywater, S. *Macromolecules* 1974, **7**, 443
6 Hadjichristidis, N. and Roovers, J. E. L. *J. Polym. Sci., Polym. Phys. Edn.* 1974, **12**, 2521
7 Bauer, B. J., Hadjichristidis, N., Fetters, L. J. and Roovers, J. E. L. *J. Am. Chem. Soc.* 1980, **102**, 2410
8 Roovers, J. E. L., Hadjichristidis, N. and Fetters, L. J. *Macromolecules* 1983, **16**, 214
9 Nguyen, A. B., Hadjichristidis, N. and Fetters, L. J. *Macromolecules* 1986, **19**, 768
10 Stivala, S. S., Khorramian, B. A. and Patel, A. *Polymer* 1986, **27**, 517
11 Huber, K., Burchard, W. and Fetters, L. J. *Macromolecules* 1984, **17**, 541
12 Mazur, J. and McCrackin, F. *Macromolecules* 1977, **10**, 326
13 Mattice, W. L. *Macromolecules* 1980, **13**, 506
14 Kolinski, A. and Sikorski, A. *J. Polym. Sci., Polym. Chem. Edn.* 1982, **20**, 3147
15 Kajiwara, K. and Burchard, W. *Macromolecules* 1982, **15**, 660
16 Zimm, B. H. *Macromolecules* 1984, **17**, 2441
17 Freire, J. J., Pla, J., Rey, A. and Prats, R. *Macromolecules* 1986, **19**, 452
18 Institut Max von Laue–Paul Langevin, 'Neutron Beam Facilities Available for Users', Jan. 1981 Edn.
19 Ghosh, R. E. 'A Computing Guide for SANS Experiments at the ILL', 1981, GH 29T
20 Huber, K., Burchard, W. and Bantle, S. *Polymer* 1987, **28**, 863 (part 1)
21 Stracielle, C. and Benoit, H. *Macromolecules* 1975, **8**, 203
22 Flory, P. J. 'Statistical Mechanics of Chain Molecules', Interscience Publishers, New York, USA (1969)
23 Yoon, D. Y. and Flory, P. J. *J. Chem. Phys.* 1974, **61**, 5366
24 Schmidt, M. and Burchard, W. *Macromolecules* 1981, **14**, 210
25 Mattice, W. L. *Macromolecules* 1975, **8**, 644
26 Mattice, W. L. and Carpenter, D. K. *Macromolecules* 1976, **9**, 53
27 Huber, K., Bantle, S., Lutz, P. and Burchard, W. *Macromolecules* 1985, **18**, 1461
28 Yamakawa, H. 'Modern Theory of Polymer Solution', Harper and Row, New York, USA (1971)
29 Burchard, W., Schmidt, M. and Stockmayer, W. H. *Macromolecules* 1980, **13**, 580
30 Vrentas, J. S., Liu, H. T. and Duda, J. C. *J. Polym. Sci., Polym. Phys. Edn.* 1980, **18**, 633
31 Kirkwood, J. G. and Riseman, J. *J. Chem. Phys.* 1948, **16**, 565
32 Berry, G. C. *J. Chem. Phys.* 1966, **44**, 4550
33 For values of $qR_g < 1$ the particle scattering factor can be well approximated by $1/P(\theta) \simeq (1 + 1/6R_g^2q^2)^2$; thus in this region the Berry plot gives a straight line. The more familiar Guinier plot yields a straight line only in a more limited range of $R_gq < 0.4$, and shows a curvature at larger R_gq values